

# THERMAL ACTIVATED COMPOSITE STRUCTURE WITH SHAPE MEMORY EFFECT

Abdul BASIT<sup>1</sup>, Gildas L'HOSTIS<sup>2</sup>, Bernard DURAND<sup>2</sup>

<sup>1</sup> Department of Yarn Manufacturing, Faculty of engineering and Technology, National Textile University, Faisalabad, Pakistan

<sup>2</sup> Laboratory of Physics and Mechanic Textiles (LPMT), University of Haute Alsace, 11 rue Alfred Werner, 68093 Mulhouse Cedex, France

Email: gildas.lhostis@uha.fr, Web Page: <http://www.uha.fr>

**Keywords:** Polymer composites, Shape memory, Thermo-mechanical, Thermal properties

## Abstract

For actuation and in various technological fields such as micro robot, space or biomechanics, the shape memory polymers and shape memory polymer (SMP) have known many developments. For a weight gain point of view, they may be substitutes for metal alloys with shape memory (SMA). However for a same level of recovery deformation, the corresponding recovery force given by SMP remains low compare to SMA, and limits the SMP actuation property. Different solutions have been explored, for example the introduction of micro or nano fillers or an elastic coupling using SMP / AMF structures leading to more efficient and having specific activation properties. In this paper, after a definition of one way or two way shape memory effect and the notions of dual, triple or multi shape, properties which characterized the nature of the SMP, we present a high rigidity shape memory composite material which have high-capacity of actuation. This composite is obtained by coupling with a thermal activation, the shape memory properties of an epoxy matrix with the morphing property of an active composite. The step of programming will be detailed. To obtain the actuation properties and from the two steps of unconstrained and constrained recovery the recovery mechanical work will be defined. Finally the structural aspects will be studied, through the influence of the organization of the constitution of the composite.

## 1. Introduction

The shape memory materials (SMM) are being mostly studied nowadays. The reason behind is their ability to return back to their original position from their fixed temporary position. Among the SMM, the shape memory polymers (SMP) or their composites are mostly being investigated under different stimuli (heat, light, electric and magnetic fields, pH, water, etc.) [1-2] These are replacing shape memory alloys as these are light weight, of low cost, demand easy fabrication etc. [3]. Currently, SMP are under consideration in terms of one step recovery [4], multi step recovery, one way effect, two way effect [5-6], three way effect [7] etc. The different functionalities based on the direction of activation and deactivation of a SMP (Fig.1) can be one-way SME or 2-way SME. Similarly, based on the different shapes, dual shape or triple shape or even multi-shapes have been defined [8]. In dual shape, the sample can have two shapes. In triple shape, it can have three shapes and similarly, in multi-shapes, it can have many shapes. For dual shape and one-way SME, the samples become active on providing stimulus and get the other shape, however, when stimulus is removed, the sample maintains this position and cannot return to the initial position. For dual shape and 2-way SME, the samples become active on providing stimulus and get the other shape, however, when stimulus is removed, the sample returns to the initial position. Hence, the sample can repeat this phenomenon on giving and removing the stimulus. For triple shape and one-way SME, the samples become active on providing stimulus and get the 1st shape. On further providing the stimulus, it gets the 2nd shape. However, when stimulus is removed, the sample maintains this position and cannot return to the 1st shape or initial position. In 2-way SME, the samples become active on providing stimulus and get the 1st shape. On further providing stimulus, it gets the 2nd shape. However, when stimulus is removed, the sample returns to the 1st shape

and then to the initial position. Hence, the sample can repeat this phenomena on providing and removing the stimuli.

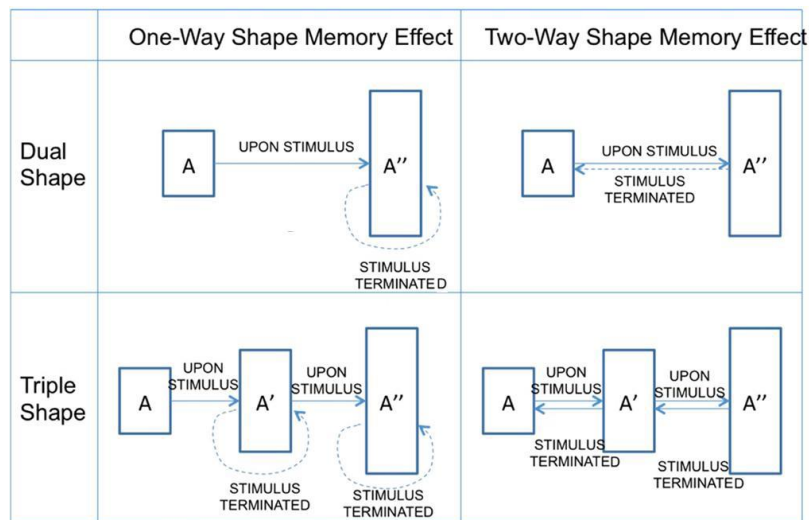


Figure 1: Functionalities of SMPs and their composites [8]

To obtain the shape memory property in SMP, it is first programmed and it is then recovered. During its programming, it is first heated (at a temperature close to its  $T_g$ ), deformed and cooled at lower temperature. As a result, a temporary shape is obtained. After that its recovery is performed during which it is heated at or below the temperature that is obtained during its programming. This recovery is executed under free condition or under constrained condition. Under free condition, the temporary shape is recovered during which the recovered strain is obtained whereas under constrained condition, the temporary shape is fixed and recovered stress is obtained [2-3, 9].

In general, SMPs have low strength and stiffness that is why they have high elongation strain. The addition of reinforcement such as carbon nano-tubes, nano-fibers, fillers, fibers or fabric layers etc. increases the stiffness and strength of the structure which ultimately influence the shape memory properties of the shape memory polymer composites. The increase in stiffness due to the reinforcement increases the elastic modulus of the structure. Hence, the instantaneous spring-back displacement increases during the programming cycle of the composite which results in decrease in overall fixity of the composite [10].

The fiber volume fraction of the reinforcement also affects the overall behavior of the shape memory composites. As fixity is obtained mainly due to the matrix in the composite, therefore, higher fiber volume fraction reduces the fixity of the composite. Moreover, more fiber volume fraction increases the recovery of the composites as the elastic recovery of the reinforcement helps in the recovery of the composites. As a result, residual strain decreases for the shape memory polymer composites with more fiber volume fraction. The residual strain decreases as a part of this residual strain is already recovered as spring-back recovery during the programming cycle [11].

In this work, we have developed a conventional shape memory composite with 2W-SME by coupling an active composite with an epoxy resin having shape memory property. The Controlled Behavior Composite Material (CBCM) is a morphing thermal active composite, based on the bimetallic strip effect, and generally asymmetric [12]. The internal heat source producing the thermal activation of the composite is generated by carbon yarns inserted in the composite, the thermal active layer AL. Like any morphing composite, the CBCM has the 2W effects corresponding to the active and non-active positions. By the thermal field the coupling between the CBCM effect and the SMP property of epoxy resins is easily obtained and controlled.

## 2. Materials and methods

The different types of rectangular plates ( $395 \times 125 \times 2 \text{ mm}^3$ ) have been made by compression moulding. The composition of the different plates is given in Figure 2. All the plates are made of six layers: two

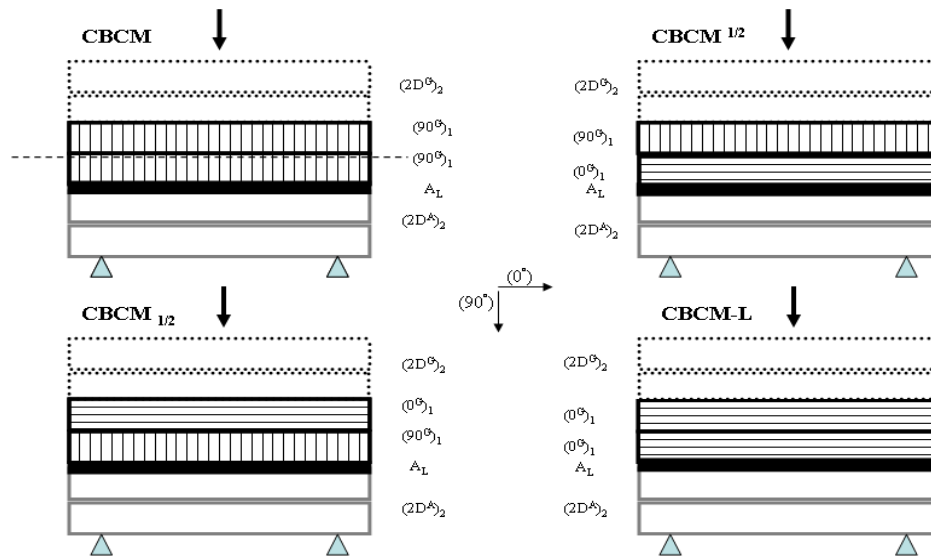


Figure 2: Organization of different asymmetric composite plates

layers of plain weave of Glass fabric ( $2D^G$ ) of  $196 \text{ g/m}^2$ , two layers of unidirectional Glass fibers ( $90^G$ ) of  $588 \text{ g/m}^2$ , the active layer ( $A_L$ ) and two layers of plain weave Aramid fabric ( $2D^A$ ) of  $173 \text{ g/m}^2$ . Note that  $0^\circ$  is along the longitudinal direction of the plate. For each composite plate, eight carbon yarns of the active layer ( $A_L$ ) are along the length of the plate ( $0^\circ$ ). The resin used is an epoxy resin (Epilam 20-25 from Axson Corporation). The curing cycle is followed, recommended by the manufactures to obtain the  $T_g$  of  $130^\circ\text{C}$ . By interdigitated electrodes, the carbon yarns of the active layer are connected to a generator of DC current. So, by Joule effect, the active layer plays a role of an internal heat source in the composite. This internal heat source is used to activate the CBCM-effect as well as to heat the composite during the programming cycle in order to obtain the shape memory property of the composite.

### 3. Experimental

#### 3.1. Experimental equipment

A three-point bending test has been chosen, the plates are supported by two rigid cylinders placed ( $L = 300 \text{ mm}$ ) apart. The thermo-mechanical cycle (Fig. 3) starts with the pretension of  $0.3 \text{ N}$  at the start of each test. Then the plate is heated for 800 seconds. The initial displacement for CBCM (free displacement  $d_A$  is equal to  $13.47 \text{ mm}$ ) shown by AB. During 800 s of heating, the deforming temperature ( $T_D$ ) is stabilized ( $T_g + 20^\circ\text{C}$ ). When temperature is stabilized, load is applied to get the specific bending deformation where  $d_S = 25 \text{ mm}$ , the total prescribed displacement (BC). This displacement is the maximum displacement that can be obtained without any delamination damage. This deformation is maintained and cooled for 1000 s to get the ambient temperature  $T_A$  (CD). When the plate becomes cooled, load is reduced to the pretension of  $0.3 \text{ N}$  (DE). Here, at point E, initial fixity is obtained. The fixing or programming cycle is thus completed. The two parts of the programming cycle can be explained in terms of different forces acting during the cycle. The total force  $F_T$  (A-A<sub>2</sub>) is the sum of two forces: the blocking force  $F_B$  (A-A<sub>1</sub>), corresponding to the active part. The force  $F_1$  (A<sub>1</sub>-A<sub>2</sub>) is imposed to reach the prescribed displacement  $d_S = 25 \text{ mm}$ . Similarly, during cooling, the total force  $F_T$  (C-C<sub>3</sub>), is the combination of three forces: the blocking force  $F_B$  (C-C<sub>1</sub>), the force  $F_S$  (C<sub>1</sub>-C<sub>2</sub>) called as force of stabilization, and the elastic force  $F_E$  (C<sub>2</sub>-C<sub>3</sub>). The blocking force  $F_B$  disappears simply due to the cooling of the composite and  $F_E$  is restituted force during the elastic recovery (DE) to the preloaded position.  $F_E$  is the result of the equilibrium of the whole structure during the unloading step. The fixity  $d_F^I$  is linked to the value of  $F_S$ . For more  $F_S$ , more will be the fixity and vice versa. So, the values of  $F_S$  and  $d_F^I$  characterize the internal mechanical work stored in the composite structure after the programming cycle.

Excerpt from ISBN 978-3-00-053387-7

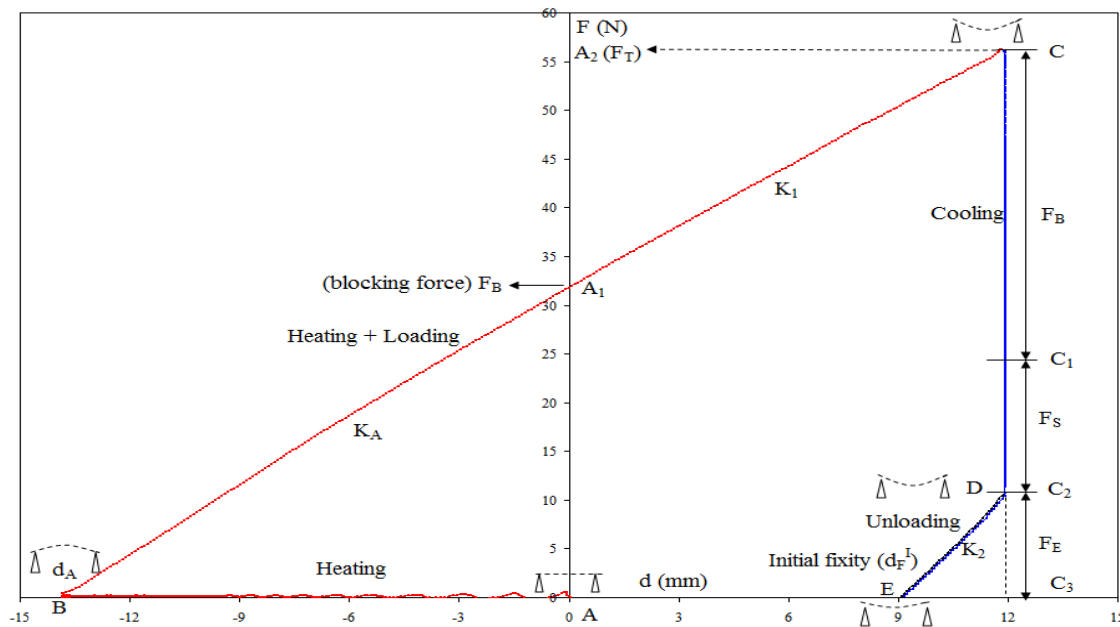


Figure 3: Thermo-mechanical programming cycle, AB = heating from 22°C to 150°C for 800 seconds, BC = 150°C maintained till required deformation, CD= cooling from 150°C to 20°C for 1000 seconds, DE = 20°C maintained.

The rigidities  $K_A$  and  $K_1$  are the characteristic behavior of the non-programmed composite plate at  $T_D$ . The rigidity  $K_2$  (DE) during unloading is the characteristic of the programmed composite plate at ambient temperature ( $T_a$ ). It can be compared to the non-active rigidity  $K_{NA}$  that is the characteristic of the non-programmed composite plate at  $T_a$ . The level of internal stress in the composite plate induced by its new shape ( $d_F^I$ ) leads to the value of  $K_2$  higher than  $K_{NA}$ .

### 3.2. Recovery test

In order to investigate the one-step recoveries of the different composites under free condition, the unconstrained recovery tests were performed by providing the recovery temperature ( $T_R$ ) equal to the deforming temperature ( $T_D = 150^\circ\text{C}$ ). During the first recovery cycle, the total recovery displacement ( $d_{RT}$ ) consists of two parts: recovery displacement due to SME ( $d_R$ ) and the free displacement ( $d_A$ ) due to the asymmetry of the composite. Similarly, two successive recovery cycles were also provided to investigate the successive deprogramming of the composites. Similarly, one-step constrained recovery tests were performed by fixing the initial fixity ( $d_F^I$ ) obtained through the programming cycle during the recovery heating at a  $T_R$  equal to  $T_D$  and recording the force generated by the plate. These constrained recoveries give a measure of the recovery forces produced for the different composites. During the heating of first recovery cycle, the total recovery force ( $F_{RT}$ ) was measured.  $F_{RT}$  is the combination of two forces: the actual recovery force ( $F_R$ ) due to the SME, and the blocking force ( $F_B$ ), produced by the asymmetry. Furthermore, in order to investigate the generation of forces during heating and residual forces ( $F_{RES}$ ) during cooling, two successive recovery cycles were given and discussed for different composites. By the curve defined from the displacement obtained from the unconstrained recovery test and the force obtained from the constrained recovery test, the maximum work produced is calculate by using the equation.

$$W_{MAX} = \frac{1}{4} F \cdot d \tag{1}$$

## 4. Results and Discussion

### 4.1. Shape memory programming of the composite

The results of CBCM at a deforming temperature  $T_D$  (i.e.  $150^\circ\text{C}$ ) have been verified at a temperature higher than  $T_g$  (Tab.1). For a given temperature, the asymmetry of the composite may be defined by the plate curvature and the value of the corresponding displacement  $d_A$ . Thus, CBCM and CBCM-L appear

to be the most and the least asymmetrical composites respectively. For the different composites, the evolution of  $F_S$  is in accordance with the evolution of  $d_A$ . This result confirms that  $F_S$  is induced by the composite asymmetry and can also be used to characterize the level of the asymmetry. Due to the lower value of  $F_E$  (the elastic force responsible for the spring-back of the composite) and despite the lower value of the total force  $F_T$ , the maximum value of  $F_T$  minus  $F_E$  is obtained for the CBCM. The direct consequence of this result is given by the value of  $d_F^I$ , CBCM has the maximum value of the  $d_F^I$ .

| Characteristic values | Composite plates |                     |                     |            |
|-----------------------|------------------|---------------------|---------------------|------------|
|                       | CBCM             | CBCM <sup>1/2</sup> | CBCM <sub>1/2</sub> | CBCM-L     |
| $d_A$ (mm)            | -13.47±0.75      | -11.64±0.27         | -9.57±0.57          | -6.81±0.35 |
| $F_B$ (N)             | 31.48±1          | 34.90±0.14          | 27.57±0.6           | 23.5±0.61  |
| $K_A$ (N/mm)          | 2.33±0.1         | 2.99±0.06           | 2.88±0.15           | 3.4±0.12   |
| $F_T$ (N)             | 57.70±1.94       | 66.61±1.06          | 69.37±0.81          | 74.80±0.86 |
| $K_1$ (N/mm)          | 2.2±0.24         | 2.25±0.08           | 2.45±0.1            | 2.67±0.05  |
| $F_S$ (N)             | 14.31±2.06       | 9.86±0.49           | 6.87±0.8            | 5.92±0.5   |
| $F_E$ (N)             | 11.91±1.62       | 21.85±0.81          | 34.93±0.67          | 45.38±0.75 |
| $d_F^I$ (mm)          | 9.18±0.63        | 8.25±0.42           | 7.08±0.48           | 6.42±0.54  |
| $K_2$ (N/mm)          | 4.24±0.39        | 3.79±0.13           | 3.7±0.1             | 3.6±0.18   |
| $K_{NA}$ (N/mm)       | 3.34±0.36        | 3.6±0.37            | 3.76±0.1            | 4.1±0.13   |

Table 1: Different characteristic values of different composites during their thermo-mechanical programming cycle

The maximum value of  $F_B$  is obtained for CBCM<sup>1/2</sup>. This result may be explained by two effects: the thermal activation and the loss of mechanical properties of the matrix because of the heat and more particularly at  $T_D=150^\circ\text{C}$ . These effects can be different depending on the reinforcement organization in the structure and particularly the orientation of the glass unidirectional layer. For the Glass unidirectional layer along the transversal direction, the higher properties of dilatation are along the longitudinal direction of the composite, but in this direction, the loss of rigidity of the matrix is also high. The competition between these two effects explains the greater value of  $F_B$  for CBCM<sup>1/2</sup>, as for the combination of these two unidirectional layers, the bottom layer at  $0^\circ$  decreases the loss of rigidity while maintaining good properties of dilatations for the two layers. For the two other composites (CBCM<sub>1/2</sub> and CBCM-L), the two unidirectional layers give lesser values of  $d_A$  and  $F_B$  due to a greater rigidity  $K_1$  at  $T_D$  and  $K_{NA}$  at  $T_A$ .

The variation of the rigidity  $K_2$  defined by  $d_F^I$  and  $F_E$  versus the asymmetry is in accordance with  $d_F^I$  and  $F_S$ ,  $K_2$  is more for more asymmetry.  $K_2$  reflects the level of internal stress in the composite after the programming cycle. So during recovery, the maximum recovery properties ( $d_R$  and  $F_R$ ) will be given by the CBCM.

#### 4.2. Unconstrained and constrained recovery

The unconstrained recoveries (Fig. 4) for the composite plates demonstrate that CBCM has highest displacement recovery as it gives highest  $d_A$  and  $d_F^I$ . The  $d_{RT}$  and the  $d_{RES}$  is more for the plate having more asymmetry. Also, the rigidities of the plates ( $K_1$ ,  $K_{NA}$ ) have a direct effect on the residual displacements after recovery. More the rigidity, less will be the  $d_{RES}$  that demonstrates that high rigidity makes the composite plate to return close to its initial position after cooling. In the representative curves of constrained recoveries (Fig. 5),  $F_{RT}$  is the sum of  $F_B$  and  $F_R$  and due to  $F_B$ , the maximum value is given by the CBCM<sup>1/2</sup>. However, like the recovery displacement  $d_R$ , the recovered force  $F_R$  is maximum for CBCM. After the cooling of the first recovery, a residual force  $F_{RES}$  remains. More the plates are rigid ( $K_1$ ,  $K_{NA}$ ), more is  $F_{RES}$ . A hypothesis was proposed to explain the existence of  $F_{RES}$  [4]. It was proposed that during the recovery heating of the constrained recovery, the level of the stress field and the reinforcement-polymer interaction affect the property of the polymer rearrangement and modify the

equilibrium between the deformation energy of the reinforcement and the polymer. The hypothesis made is confirmed by the values of  $F_{RES}$  obtained for the different asymmetrical composites. During the recovery heating to  $T_R = 150^\circ\text{C}$  and cooling to  $T_A$ , the plate remains fixed and immovable.

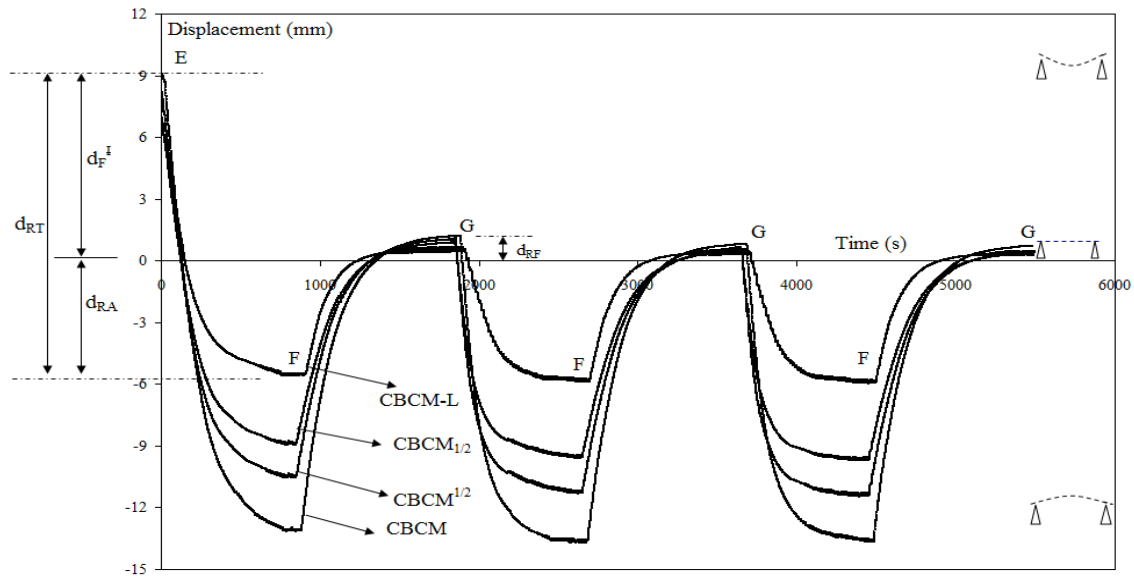


Figure 4: Unconstrained recovery for different CBCM; E= Initial fixities; EF, GF = Heating to  $T_D$  (i.e. =  $150^\circ\text{C}$ ); FG = Cooling to  $T_A$  (i.e. =  $22^\circ\text{C}$ );  $d_F^I$  for CBCM,  $\text{CBCM}^{1/2}$ ,  $\text{CBCM}_{1/2}$ , and CBCM-L are  $9.18 \pm 0.63$  mm,  $8.25 \pm 0.42$  mm,  $7.08 \pm 0.48$  mm and  $6.42 \pm 0.54$  respectively

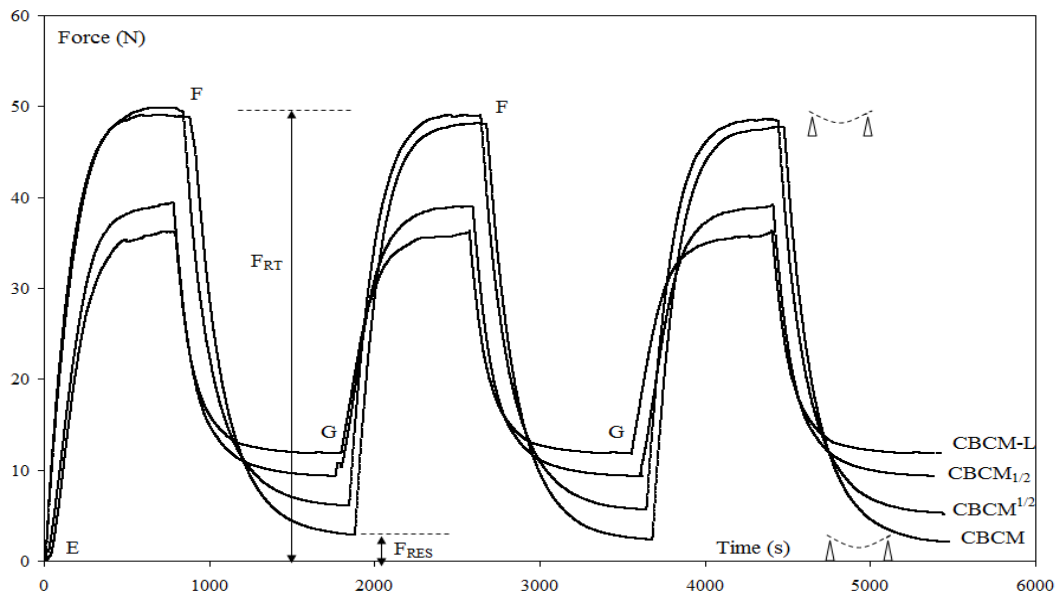


Figure 5: Constrained recovery ( $F_{RT}$ ) for different CBCM composites; E= Initial fixities; EF, GF = Heating to  $T_D$  (i.e. =  $150^\circ\text{C}$ ); FG = Cooling to  $T_A$  (i.e. =  $22^\circ\text{C}$ );  $d_F^I$  for CBCM,  $\text{CBCM}^{1/2}$ ,  $\text{CBCM}_{1/2}$ , and CBCM-L are  $9.12 \pm 0.3$  mm,  $8.25 \pm 0.42$  mm,  $7.08 \pm 0.48$  mm and  $6.42 \pm 0.54$  respectively

So,  $F_{RES}$  is linked to the ability of the polymer (at  $T_R$ ) to reorganize and return to its initial configuration (before the programming cycle).

- If the polymer can rearrange and recovers to its initial configuration, the equilibrium between the deformation energy of the reinforcement and the polymer is largely modified, the value of  $F_{RES}$  is high, and  $\delta F$  will be low (close to zero).

- If the polymer cannot rearrange to its initial configuration, the equilibrium between the deformation energy of the reinforcement and the polymer change to a smaller extent. So, the polymer again acts as a lock and thus will maintain the reinforcement position. Hence,  $F_{RES}$  is low and  $\delta F$  will be high.

The polymer rearrangement is linked to the level of stress in the polymer, and consequently to the stress transfer between fiber and matrix in the layers and at the interfaces. For the unidirectional layers of CBCM, the flexural stress is distributed mainly on the polymer, thus, limiting its ability to reorganize. For the other composites, more is the rigidity ( $K_I$ ,  $K_{NA}$ ), more the flexural stress will be supported by the fibers, and more the polymer can rearrange during the recovery heating in the composite structure. Thus, the equilibrium between polymer and reinforcement is modified, the plate is partially deprogrammed and the strength of the actuation is less.

| Composite plates    | Force (N)                     | Recovery cycles |            |            |
|---------------------|-------------------------------|-----------------|------------|------------|
|                     |                               | 1               | 2          | 3          |
| CBCM                | $F_{RT}$                      | 48.54±1.57      | 47.77±1.37 | 47.44±1.33 |
|                     | $F_{RES}$                     | 3.03±0.96       | 2.51±0.87  | 2.23±0.94  |
|                     | $\delta F = F_{RT} - F_{RES}$ | 45.51±0.61      | 45.26±0.5  | 45.21±0.39 |
| CBCM <sup>1/2</sup> | $F_{RT}$                      | 49.30±0.93      | 48.71±0.84 | 48.30±0.7  |
|                     | $F_{RES}$                     | 6.01±0.5        | 5.57±0.3   | 5.16±0.45  |
|                     | $\delta F = F_{RT} - F_{RES}$ | 43.29±0.43      | 43.14±0.65 | 43.14±0.25 |
| CBCM <sub>1/2</sub> | $F_{RT}$                      | 39.70±0.8       | 39.37±0.9  | 39.13±0.95 |
|                     | $F_{RES}$                     | 9.31±0.57       | 8.83±0.52  | 8.73±0.61  |
|                     | $\delta F = F_{RT} - F_{RES}$ | 30.39±0.23      | 30.54±0.38 | 30.4±0.34  |
| CBCM-L              | $F_{RT}$                      | 35.43±0.81      | 34.98±0.97 | 34.60±0.48 |
|                     | $F_{RES}$                     | 12.87±0.64      | 12.47±0.45 | 12.23±0.77 |
|                     | $\delta F = F_{RT} - F_{RES}$ | 22.56±0.17      | 22.51±0.52 | 22.37±0.29 |

Table 2: Forces produced during constrained recoveries of different composites

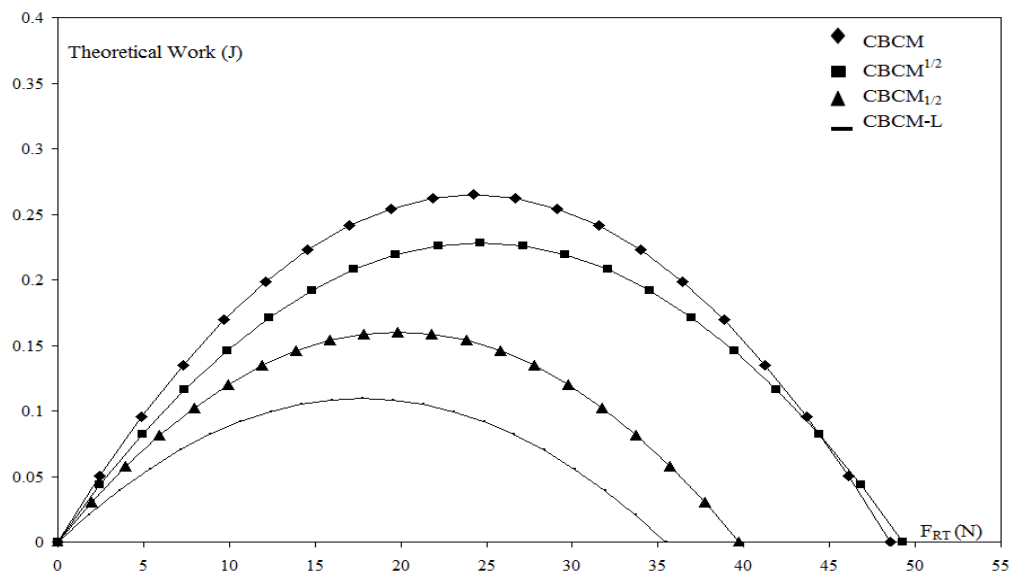


Figure 6: Theoretical work for different composites

#### 4.3. Characteristic straight lines and theoretical work

The maximum theoretical work (Fig. 6) given by  $d_{RT}$  and  $F_{RT}$  calculated by using the Eq. 1, is observed, it is found that it is maximum for CBCM (0.265 J) and minimum for CBCM-L (0.1 J) as CBCM has the

highest CBCM-effect (maximum asymmetry) and CBCM-L has the least CBCM-effect (minimum asymmetry). For CBCM<sup>1/2</sup> it is 0.228 J, for CBCM<sub>1/2</sub> it is 0.16 J.

Similarly, for the SME, the maximum work calculated by  $F_R$  and  $d_R$  by using Eq. 2 for CBCM, CBCM<sup>1/2</sup>, CBCM<sub>1/2</sub>, and CBCM-L are 0.035 J, 0.0248 J, 0.02 J, 0.016 J respectively. It can be observed that the work induced by SME is the least for CBCM-L; however, it is maximum for CBCM. This shows that the actuation strength of the composite strongly depends upon the SME in which the rigidity  $K_{NA}$  plays an important role.

## 5. Conclusions

The study of the effect of change in position and orientation of unidirectional glass layers in the composite changes the asymmetry of the composite which ultimately affect all its characteristic parameters. The change in asymmetry changes not only the free displacement and blocking force but also changes the shape memory properties of the composite. The greater asymmetry of the composite will give better shape memory properties. The initial fixity is degraded as the rigidity of the composite increases with the change of position and orientation of unidirectional glass layers in the composite. More the rigidity more will be the elastic recovery during programming, however; lesser will be the stored strain. As a result, the recovered work is also affected. Furthermore, it is found that the force of stabilization is the measure of the asymmetry of the composite. In addition, the composite having more asymmetry gives higher actuation properties than the other composites.

## References

- [1] K. Fan, W. M. H., C. C. Wang, Z. Ding, Y. Zhao, H. Purnawali, K .C. Liew, L. X. Zheng, "Water-responsive shape memory hybrid: Design concept and demonstration," *eXPRESS Polymer Letters*, vol. 5, pp. 409–416, 2011.
- [2] Sun, L., Huang W. M., Ding Z., Zhao Y., Wang C. C., Purnawali H. and Tang C., "Stimulus-responsive shape memory materials: A review," *Materials & Design*, vol. 33, pp. 577-640, 2012.
- [3] Hu, J., Zhu Y., Huang H. and Lu J., "Recent advances in shape-memory polymers: Structure, mechanism, functionality, modeling and applications," *Progress in Polymer Science*, vol. 37, pp. 1720-1763, 2012.
- [4] Basit, A., L'Hostis G. and Durand B., "High actuation properties of shape memory polymer composite actuator," *Smart Materials and Structures*, vol. 22, p. 025023, 2013.
- [5] Basit, A., LHostis G., Pac M. and Durand B., "Thermally Activated Composite with Two-Way and Multi-Shape Memory Effects," *Materials*, vol. 6, pp. 4031-4045, 2013.
- [6] Basit, A., L'Hostis G. and Durand B., "Multi-shape memory effect in shape memory polymer composites," *Materials Letters*, vol. 74, pp. 220-222, 2012.
- [7] H. Tobushi, S. H., E. Pieczynska, K. Date, Y. Nishimura, "Three-way actuation of shape memory composite," *Archives of Mechanics*, vol. 63, 2011.
- [8] J. Leng et al., Shape memory polymers and their composites: stimulus methods and applications, *Progress in Materials sciences*, vol.56, pp1077-1135, 2011.
- [9] Q. Meng, J.Hu., "A review of shape memory polymer composites and blends," *Composites Part A: Applied Science and Manufacturing*, vol. 40, pp. 1661-1672, 2009.
- [10] Nishikawa, M., Wakatsuki K., Yoshimura A. and Takeda N., "Effect of fiber arrangement on shape fixity and shape recovery in thermally activated shape memory polymer-based composites," *Composites Part A: Applied Science and Manufacturing*, vol. 43, pp. 165-173, 2012.
- [11] Ohki, T., Ni Q.-Q., Ohsako N. and Iwamoto M., "Mechanical and shape memory behavior of composites with shape memory polymer," *Composites Part A: Applied Science and Manufacturing*, vol. 35, pp. 1065-1073, 2004.
- [12] Gautier, K. B., L'Hostis G., Laurent F. and Durand B., "Mechanical performances of a thermal activated composite," *Composites Science and Technology*, vol. 69, pp. 2633-2639, 2009